

# Barium Isotopes in Cold-Water Corals

Freya Hemsing<sup>a,b\*</sup>, Yu-Te. Hsieh<sup>b</sup>, Luke Bridgestock<sup>b</sup>, Peter T. Spooner<sup>c, 1</sup>, Laura F. Robinson<sup>c</sup>, Norbert Frank<sup>a</sup>, Gideon M. Henderson<sup>b</sup>

\*Corresponding author; [freya.hemsing@iup.uni-heidelberg.de](mailto:freya.hemsing@iup.uni-heidelberg.de)

<sup>a</sup> Institute of Environmental Physics, Heidelberg University, Im Neuenheimer Feld 229, 69120 Heidelberg, Germany

<sup>b</sup> Department of Earth Sciences, University of Oxford, South Parks Road, Oxford, OX1 3AN, UK

<sup>c</sup> School of Earth Sciences, University of Bristol, Queens Rd., Bristol, BS8 1RJ, UK

**Keywords:** Barium isotope fractionation, cold-water corals, calibration, Ba/Ca, paleoceanography

## Abstract

Recent studies have introduced stable Ba isotopes ( $\delta^{138/134}\text{Ba}$ ) as a novel tracer for ocean processes. Ba isotopes could potentially provide insight into the oceanic Ba cycle, the ocean's biological pump, water-mass provenance in the deep ocean, changes in activity of hydrothermal vents, and land-sea interactions including tracing riverine inputs. Here, we show that aragonite skeletons of various colonial and solitary cold-water coral (CWC) taxa record the seawater (SW) Ba isotope composition. Thirty-six corals of eight different taxa from three oceanic regions were analysed and compared to  $\delta^{138/134}\text{Ba}$  measurements of co-located seawater samples. Sites were chosen to cover a wide range of temperature, salinity, Ba concentrations and Ba isotope compositions. Seawater samples at the three sites exhibit the well-established anti-correlation between Ba concentration and  $\delta^{138/134}\text{Ba}$ . Furthermore, our data set suggests that Ba/Ca values in CWCs are linearly correlated with dissolved [Ba] in ambient seawater, with an average partition coefficient of  $D_{\text{CWC/SW}} = 1.8 \pm 0.4$  (2SD). The mean isotope fractionation of Ba between seawater and CWCs  $\Delta^{138/134}\text{Ba}_{\text{CWC-SW}}$  is  $-0.21 \pm 0.08\text{‰}$  (2SD), indicating that CWC aragonite preferentially incorporates the lighter isotopes. This fractionation likely does not depend on temperature or other environmental variables, suggesting that aragonite CWCs could be used to trace the Ba isotope composition in ambient seawater. Coupled [Ba] and  $\delta^{138/134}\text{Ba}$  analysis on fossil CWCs has the potential to provide new information about past changes in the local and global relationship between [Ba] and  $\delta^{138/134}\text{Ba}$  and hence about the operation of the past global oceanic Ba cycle in different climate regimes.

## 1. Introduction

Aragonitic scleractinian cold-water corals (CWC) are distributed throughout the global oceans in waters ranging from just a few meters to abyssal depths of several thousand meters (Roberts et al., 2006). In contrast to traditional paleoceanographic archives such as sediment cores, reconnaissance and precise dating of CWCs is performed by  $^{14}\text{C}$  and U-series dating (Mangini et al., 1998; Cheng et al., 2000; Douville et al., 2010; Margolin et al., 2014; Spooner et al., 2016). With linear extension rates of several mm/a (e.g. Mortensen, 2001; Orejas et al., 2008) oceanic changes on centennial, decadal, yearly or even seasonal time scales can be elucidated from geochemical and isotope tracers in aragonite CWC skeletons. Despite this advantage, only a small number of paleoceanographic tracers have been established successfully and applied in CWCs (Robinson et al., 2014). For example, temperature, state of ventilation and water-mass provenance have been retrieved from various elemental and isotope tracers (Robinson et al., 2014). However, biological factors, so-called 'vital effects', often alter some elemental and isotope systems, e.g.  $\delta^{13}\text{C}$ ,  $\delta^{18}\text{O}$  or Li/Ca, limiting their use as oceanic tracers (Adkins et al., 2003; Rollion-Bard et al., 2009; Raddatz et al., 2013).

Barium has an enigmatic oceanic chemistry that has been studied for many years. The nutrient-like distribution of dissolved Ba in seawater,  $[\text{Ba}]_{\text{sw}}$ , is closely correlated with silicate and alkalinity ( $\text{Si}(\text{OH})_4$ ) (Chow and Goldberg, 1960; Wolgemuth and Broecker, 1970; Jeandel et al., 1996). But numerous studies suggested that the oceanic Ba cycle is not directly linked to the silicate or carbonate cycle (Bishop, 1988; Monnin et al., 1999). While regenerative dissolved Ba enriches deep ocean concentrations, its removal in the upper ocean is attributed to the precipitation of barite ( $\text{BaSO}_4$ ), even though seawater is mostly under-saturated in  $\text{BaSO}_4$ . This behaviour can possibly be explained by the decay of organic matter in settling particles releasing Ba and/or  $\text{SO}_4^{2-}$  into a microenvironment until a  $\text{BaSO}_4$ -saturation is reached (Dehairs et al., 1980; Bishop, 1988; Paytan and Griffith, 2007; Horner et al., 2017).

A new-found ability to precisely measure naturally occurring fractionation between Ba isotopes enables further insight to be gained into the processes controlling the Ba cycle in the ocean. The isotope composition of Ba is defined with reference to the SRM NIST 3104a standard as

$$\delta^{138/134}\text{Ba}_{\text{NIST3104a}} = ((^{138}\text{Ba}/^{134}\text{Ba}_{\text{sample}})/(^{138}\text{Ba}/^{134}\text{Ba}_{\text{NIST3104a}}) - 1) \times 1000 \quad (1)$$

which we abbreviate to  $\delta^{138/134}\text{Ba}$ . Recent Ba isotope studies have focussed on fractionation processes during experimental precipitation of  $\text{BaCO}_3$ ,  $\text{BaSO}_4$  and  $\text{BaMn}[\text{CO}_3]_2$  (von Allmen et al., 2010; Böttcher et al., 2012; Mavromatis et al., 2016; van Zuilen et al., 2016), in igneous rocks (Miyazaki et al., 2014; Nan et al., 2015), in sediments and soils (Bridgestock et al., 2018; Bullen and Chadwick, 2016), and in seawater (Horner et al., 2015; Cao et al., 2016; Bates et al., 2017; Hsieh and Henderson, 2017). During barite,  $\text{BaCO}_3$  and  $\text{BaMn}[\text{CO}_3]_2$  precipitation experiments, the solid phase preferentially incorporates the lighter isotopes, leaving the solution relatively heavy in Ba isotopes (von Allmen et al., 2010; Böttcher et al., 2012; van Zuilen et al., 2016). Upper ocean barite formation and its dissolution in the deep ocean lead to an inverse profile for Ba isotopes compared to dissolved Ba concentration, with light Ba isotope compositions in the deep ocean and heavier isotope compositions in surface waters (e.g. Horner et al., 2015). Further studies on Ba isotopes highlighted the potential to provide insight into the oceanic Ba cycle, the ocean's biological pump, deep water-mass provenance (Bates et al., 2017; Horner et al., 2015), riverine inputs (Cao et al., 2016), and possibly other inputs from sediment and/or hydrothermal inputs (Hsieh and Henderson, 2017). To investigate past changes in these processes, CWCs could be a promising archive.

Over the years, several studies have shown that, the Ba/Ca ratio in foraminifera and calcitic corals reflects Ba concentrations in ambient seawater  $[\text{Ba}]_{\text{sw}}$  (LaVigne et al., 2011; Lea and Boyle, 1993). Recently, calibration of the Ba/Ca in aragonitic CWCs to reconstruct past  $[\text{Ba}]_{\text{sw}}$  has been a focus of research (Anagnostou et al., 2011; LaVigne et al., 2016; Spooner, 2016). However, only one study has included an assessment of Ba isotopes in coralline carbonate (Pretet et al., 2016). That study measured Ba isotopes in cultured tropical aragonitic scleractinian corals grown in Mediterranean seawater, revealing a variable fractionation (see EQ.2) between seawater and cultured coralline aragonite ranging from  $-0.02\text{‰}$  (*Acropora sp.* and *Porite sp.*) to  $-0.35\text{‰}$  (*Stylophora sp.* and *Montipora sp.*). The Ba isotope composition of natural CWCs was also reported; two *Lophelia pertusa* (*L. pertusa*) samples from the Norwegian shelf were analysed and found to have  $\delta^{138/134}\text{Ba}$  values of  $0.25 \pm 0.11\text{‰}$  and  $0.3 \pm 0.11\text{‰}$ .

In this study we present the first detailed study of  $\delta^{138/134}\text{Ba}$  in natural CWCs in comparison to that of the seawater in which they grew. The data set includes thirty-six well-characterised aragonitic

scleractinian specimens from eight different taxa, both solitary and colonial, recovered from three sites: the North Atlantic, the Equatorial Atlantic, and the Drake Passage. The samples cover a wide range of environmental conditions, Ba concentrations, and seawater Ba isotope compositions. This allows for a systematic assessment of the Ba isotope fractionation during coral growth and the use of CWCs as an archive for past seawater  $\delta^{138/134}\text{Ba}$ .

## 2. Materials and analytical methods

### 2.1 Samples

Thirty-six CWCs and ambient seawater samples from three ocean regions were selected for Ba isotope analysis. The locations were: south of Iceland in the North Atlantic (Reykjanes Ridge and Hafadjup), in the Equatorial Atlantic (Carter Seamount), and in the Drake Passage (Burdwood Bank) (Tab.1). They were chosen to cover a wide range of temperature and salinity (e.g. T: 2 – 11.5°C; S: 34.29 – 35.32 psu), Ba concentrations and Ba isotope compositions (Fig. 1, 2 & 7, supplementary material). Eight different colonial and solitary aragonite scleractinian coral taxa (identified to either genus or species level) of living or young (less than 1000 a) CWCs were sampled: *Lophelia pertusa* (*L. pertusa*), *Madrepora oculata* (*M. oculata*), *Desmophyllum dianthus* (*D. dianthus*), *Balanophyllia* sp., *Caryophyllia* sp., *Dasmomillia* sp., *Flabellum* sp. and *Javania* sp. (supplementary material). Corals off Iceland were collected during the ICECTD cruise in 2012 (Frank et al., 2012) using the ROV Victor 6000 (provided by IFREMER). Simultaneously, seawater samples (125 ml) were directly filled (unfiltered) into acid cleaned PEP bottles by the ROV. They were stored at room temperature. Three months prior to Ba isotope analysis, seawater samples were acidified to a pH of 1.5 by adding purified, concentrated HCl. Therefore, in these samples total dissolvable Ba concentrations and isotope compositions are analysed. Equatorial Atlantic samples from Carter Seamount were recovered during the JC094 cruise in 2013 (Robinson, 2014; Spooner et al., 2016). The corals were collected by the ROV *Isis*. Ambient seawater samples are from CTD station 2 and were analysed by Bates et al., 2017. In contrast to seawater samples from Iceland and the Drake Passage, Equatorial Atlantic samples were filtered with 0.4  $\mu\text{m}$  Acropak cartridge filters before acidification. CWCs from Burdwood Bank in the Drake Passage were collected

in 2011 during cruise NBP1103, using a small basket dredge and trawls (Chen et al., 2015; Margolin et al., 2014; Robinson and Waller, 2011). Depths and coordinates given here are the average for each retrieval event. Seawater samples are from CTD station 21 and were taken unfiltered in Niskin bottles, acidified with 4 ml concentrated HCl and stored at room temperature. As Burdwood Bank is positioned north of the Subantarctic front an additional unfiltered seawater profile close to Sars Seamount between the Subantarctic and the Polar front was analysed (cruise NBP1103, station 100). Temperature and salinity were determined following Spooner et al. (2016). Further details regarding the coral samples are summarised in the supplementary material.

## **2.2 Ba extraction and analysis**

All samples (corals and seawater), except for the seawater samples analysed by Bates et al., 2017 (CTD 2, cruise JC094), were prepared and analysed at the Earth Sciences Department of the University of Oxford. Ba isotopes, for both seawater and CWC samples, were measured on a thermal ionisation mass spectrometer (TIMS; Thermo Scientific Triton), using a  $^{137}\text{Ba}$ - $^{135}\text{Ba}$  double spike to correct for mass fractionation during the chemical procedure and instrumental analysis (Hsieh and Henderson, 2017). For seawater analyses, about 50 ml of seawater was precisely weighed and spiked with a known quantity of the double spike. After an equilibration period of 24h, 3 ml of 0.9M  $\text{Na}_2\text{CO}_3$  solution was added to co-precipitate Ba with  $\text{CaCO}_3$ . The precipitate was centrifuged and cleaned with MilliQ water. After dissolving the precipitate in HCl, column separation was applied twice using the cation exchange resin AG50-X8 (200 – 400mesh) to purify Ba from the matrix elements (Table S2 and S3 in supplementary material of (Bridgestock et al., 2018) after (Horner et al., 2015; Foster et al., 2004; Nan et al., 2015)). To remove organics leached from the resin, 7.5M  $\text{HNO}_3$  and 9.8M  $\text{H}_2\text{O}_2$  were alternately added to the samples and evaporated. This procedure was repeated three times.

CWC samples were rinsed with fresh water on-board ship. Living corals were bleached to remove external organic tissue and washed again in fresh water. All corals were dried and stored at room temperature until analysis. The cleaning procedure was adapted from Copard et al. (2010) and Pretet et al. (2016). CWCs were thoroughly mechanically cleaned using a dremel tool, removing FeMn-coatings

and organic residues. To remove any further contamination coral pieces were then washed three times in MilliQ water in acid cleaned Teflon vials and leached in very dilute HCl. Leaching was performed by covering the sample with MilliQ water and adding drops of 2M HCl until small bubbles could be seen around the aragonite. Leaching lasted for five minutes before rinsing three times with MilliQ water again. Afterwards, samples were dried and weighed (45 – 70 mg). The sample size was chosen to have more than 300 ng of Ba for isotope measurements. Although small intra-skeletal variabilities of around 11% were observed for the aragonitic CWC species *L. pertusa* between theca walls and centres of calcification (Raddatz et al., 2016), sample size tests on two *Desmophyllum* (5-40 mg) showed that different sizes did not affect the obtained Ba/Ca result significantly and tended towards better reproducibilities for larger CWC pieces (Spooner, 2016). Therefore, the sample size used here potentially reduces the small influence of intra-skeletal Ba/Ca variability. Coral pieces were dissolved in 5 ml 7.5M HNO<sub>3</sub> and spiked with a known quantity of <sup>137</sup>Ba-<sup>135</sup>Ba double spike (Hsieh and Henderson, 2017). To ensure spike equilibration, samples were heated to 90 – 100°C for at least 12h following spike addition. Coral samples were subsequently dried down, dissolved in 3M HCl, dried again and redissolved in 1 ml 3M HCl. Ba purification by cation exchange chromatography followed the procedure for seawater samples (Table S2 and S3 in supplementary material of (Bridgestock et al., 2018)).

At least two total procedural blanks were determined alongside each batch of samples processed through the chemical separation procedure. For seawater samples these were between 0.19 and 1.6 ng (n=4), representing a maximum of 0.16% of Ba processed in samples. Most of the Ba blank is added with the Na<sub>2</sub>CO<sub>3</sub> used for co-precipitation, so blanks for coral samples processed without this step were significantly lower: 0.02 – 0.24 ng (n=5) accounting for a maximum of 0.02% of the total Ba processed in samples. Therefore, no blank correction was applied to either seawater or coral samples.

Purified samples were dissolved in 1 – 2 µl 2M HCl and loaded on a previously outgassed single Re filament, adding 1 – 2 µl Ta<sub>2</sub>O<sub>5</sub>-H<sub>3</sub>PO<sub>4</sub> activator (Hsieh and Henderson, 2017). To stabilise the ion beams during the analysis the activator was loaded on the filament prior to the samples.

For coral samples, typical ion beams during the analysis on the TIMS were 8 – 10 V for <sup>138</sup>Ba<sup>+</sup>. Seawater samples yielded slightly smaller Ba beams of 3 – 7 V <sup>138</sup>Ba<sup>+</sup> and frequently showed a less stable signal.

Seven Faraday cups simultaneously detected the masses  $138^+$ ,  $137^+$ ,  $136^+$ ,  $135^+$ ,  $134^+$ ,  $140^+$  and  $139^+$ , with the latter reflecting  $^{140}\text{Ce}^+$  and  $^{139}\text{La}^+$ , which were monitored to account for possible isobaric interferences on  $^{136}\text{Ba}$  and  $^{138}\text{Ba}$ . No  $140^+$  and  $139^+$  signals were detected above background during any analysis. A single analysis consisted of 54 blocks, each containing 10 isotope ratio measurements, with a measurement integration time of 8.4s. To monitor the electronic baseline the X-Symmetry of the instrument was adjusted to divert the ion beams before each block. Blank analyses were measured for 20 – 30 blocks. To correct for instrumental mass bias using the double spike composition, all raw data were processed offline (Hsieh and Henderson, 2017). The isotope analysis together with the known spike mass also provide Ba concentration measures. The standard JCp-1, consisting of powdered coral (Okai et al., 2002), was also analysed three times. It was prepared in the same way as CWCs samples but without the mechanical and chemical cleaning steps.

## 3 Results

### 3.1 Reproducibility

Repeat analyses of the SRM NIST 3104a standard using similar beam sizes for seawater samples lead to a long-term external reproducibility of  $\pm 0.03\text{‰}$  (2SD; (Bridgestock et al., 2018; Hsieh and Henderson, 2017)). Repeat analysis of the coral standard JCp-1 yielded a  $\delta^{138/134}\text{Ba}$  of  $0.25 \pm 0.03\text{‰}$  (2SD,  $n=3$ ), which is within error of analyses in two other laboratories with values of  $0.29 \pm 0.03\text{‰}$  (Horner et al., 2015) and  $0.26 \pm 0.1\text{‰}$  (Pretet et al., 2016). Several duplicates of seawater and coral samples confirm the reproducibility of  $\pm 0.03\text{‰}$  (supplementary material). Bridgestock et al., (2018) and Hsieh and Henderson (2017), studies also undertaken at University of Oxford, further verify this level of reproducibility for seawater and sediment samples. Two analyses were discarded because they yielded a larger internal standard error for  $\delta^{138/134}\text{Ba}$  than the standard reproducibility ( $\pm 0.03\text{‰}$ ) and were considered unreliable. Both of these samples were subsequently successfully re-analysed. The reproducibility for the Ba concentration of the repeated coral standard (JCp-1) and seawater sample measurements (Bridgestock et al., 2018; Hsieh and Henderson, 2017) was  $\pm 2$  to  $3\%$  (1SD), which is presumably dominated by weighing uncertainties (2 – 3%) and taken as the uncertainty for Ba

concentrations of corals and seawater measured in this study. Converting the concentration to Ba/Ca by assuming a Ca concentration of 40% per mass of the coral (Roberts et al., 2009), the average Ba/Ca in JCp-1 obtained in this study,  $7.94 \pm 0.22 \mu\text{mol/mol}$  ( $n=3$ ; 3% 2SD), is within uncertainty of previous studies (e.g.  $7.465 \pm 0.655$ ; (Hathorne et al., 2013)). For seawater samples a Ca concentration of 10.3 mmol/kg (Henderson and Henderson, 2009) was taken to convert Ba concentrations into Ba/Ca<sub>sw</sub> values.

### 3.2 $\delta^{138/134}\text{Ba}$ in seawater profiles

The seawater profile from the Burdwood Bank in the Drake Passage shows the established anti-correlation between [Ba]<sub>sw</sub> and  $\delta^{138/134}\text{Ba}$  (Fig. 1; (Bridgestock et al., 2018; Hsieh and Henderson, 2017; Bates et al., 2017; Pretet et al., 2016; Horner et al., 2015)). Note, that seawater data from the South China Seas were reported to exhibit a different correlation between [Ba]<sub>sw</sub> and  $\delta^{138/134}\text{Ba}$  (Cao et al., 2016) and were therefore excluded in the compilation of published data (Fig. 1). [Ba]<sub>sw</sub> is 55.2 nmol/kg in surface waters and increases to 102 nmol/kg at 2250 m water depth. The isotope composition of Ba decreases with depth from 0.5‰ to 0.25‰.

Tropical Atlantic water samples measured and described in detail by Bates et al. (2017) (CTD 2, cruise JC094) show a similar distribution with Ba concentrations increasing from 37.9 (11 m) to 84.6 nmol/kg at 4512 m depth and  $\delta^{138/134}\text{Ba}$  decreasing from 0.57‰ to 0.31‰ (Fig. 1). Note, that Ba concentration for station CTD 2 were initially given in nM (Bates et al., 2017) and have been recalculated here to nmol/kg by assuming a seawater density of 1.027 kg/l.

Seawater samples from south of Iceland, at Reykjanes Ridge and within Hafad Jup basin, cover the depth range of 238 to 680 m, coinciding with the depths of coral retrieval (Fig. 1). Over this depth interval both [Ba]<sub>sw</sub> and  $\delta^{138/134}\text{Ba}$  are nearly constant within uncertainties: 49.3 – 52.9 nmol/kg and 0.51 – 0.53‰ respectively.

The seawater samples analysed in this study cover nearly the total range of presently available seawater  $\delta^{138/134}\text{Ba}$  and confirm published data (Fig. 2; (Bridgestock et al., 2018; Hsieh and Henderson, 2017; Bates et al., 2017; Pretet et al., 2016; Horner et al., 2015)). Isotope compositions of Ba from publications originally reporting in  $\delta^{137/134}\text{Ba}$  were converted to  $\delta^{138/134}\text{Ba}$  by multiplying by a factor of 1.3 (after



Horner et al.; 2015). The closest seawater profiles were used to compare seawater  $\delta^{138/134}\text{Ba}$  with the coral analyses. To obtain  $\delta^{138/134}\text{Ba}_{\text{sw}}$  at the water depths in which the analysed corals grew, the values of seawater samples at adjacent depths were linearly interpolated.

### 3.3 Ba/Ca in cold-water corals

Ba/Ca for corals varied between 7.5 and 16.3  $\mu\text{mol/mol}$  (Fig. 3a, supplementary material), while seawater samples spanned 3.9 to 9.7  $\mu\text{mol/mol}$  (Fig. 3a, supplementary material). Ba/Ca results of different discrete subsamples of some corals from the Equatorial Atlantic and the Drake Passage and analysis of JCp-1 ( $6.96 \pm 0.08$  2SE,  $n=13$ ) were also carried out in the Bristol Isotope Group (Spooner, 2016). Accounting for analytical deviations between the laboratories seen in the JCp-1 analysis, the measurements of both laboratories agree for all subsampled corals, despite the use of two different measurement approaches. The double spike method with Ba purification used here, analysed on a TIMS, was compared to direct Ba/Ca measurements of dissolved coral fragments using a ThermoFinnigan Element 2 ICP-MS (Spooner, 2016).

A linear least squares regression gives  $\text{Ba/Ca}_{\text{CWC}} = 1.8 (\pm 0.4, 2\text{SE}) \text{ Ba/Ca}_{\text{sw}} + 0.7 (\pm 2.6)$  with a correlation factor of  $r^2 = 0.67$ . Therefore, the overall partition coefficient  $D_{\text{CWC/SW}}(\text{Ba})$  (i.e.  $\text{Ba/Ca}_{\text{CWC}}/\text{Ba/Ca}_{\text{sw}}$ ) observed is  $1.8 \pm 0.4$  (2SE). The partition coefficient calculated separately for each CWC in this study covers a range from 1.5 to 2.4.

### 3.4 $\delta^{138/134}\text{Ba}$ in cold-water corals

CWCs of four different taxa were analysed from Burdwood Bank (Fig. 3b – 6, supplementary material). Taxa from Burdwood Bank included five *Balanophyllia* sp., two *Flabellum* sp., two *Caryophyllum* sp. and three *D. dianthus*, with samples taken from depths ranging from 334 to 1829 m. Isotope compositions  $\delta^{138/134}\text{Ba}$  are 0.24‰ in shallow corals and 0.03‰ in the deeper corals (Fig. 4), reflecting the decrease in seawater  $\delta^{138/134}\text{Ba}$  with depth. At each depth, coral  $\delta^{138/134}\text{Ba}$  values agree with each other within external reproducibility ( $\pm 0.03\%$ ), regardless of species.

The fractionation of Ba between corals and seawater can be expressed by the isotope fractionation factor  $\alpha = R_{\text{CWC}}/R_{\text{sw}}$  or the enrichment factor

$$\varepsilon = (\alpha - 1) \times 1000 \approx \Delta^{138/134}\text{Ba}_{\text{CWC-SW}} = \delta^{138/134}\text{Ba}_{\text{CWC}} - \delta^{138/134}\text{Ba}_{\text{SW}} \quad (2)$$

with an external analytical 2SD of  $\pm 0.04\text{‰}$  propagated from the analytical 2SD of  $\delta^{138/134}\text{Ba}$  ( $\pm 0.03\text{‰}$ ). Individual enrichment factors in CWCs from Burdwood Bank range from  $-0.19$  to  $-0.29\text{‰}$  with an average of  $-0.24 \pm 0.06\text{‰}$ . The uncertainty of the average is assumed to be the larger of either the propagated external reproducibility or the 2SD obtained when averaging over a number of corals. Taxa analysed from Carter Seamount include two *Dasmosillia sp.*, six *Caryophyllia sp.*, and four *Javania sp.* covering water depths from 265 to 2318m.  $\delta^{138/134}\text{Ba}$  varies from  $0.18$  to  $0.40\text{‰}$  associated with enrichment factors of  $-0.16$  to  $-0.27\text{‰}$ , with a mean of  $-0.19 \pm 0.07\text{‰}$ . Corals analysed from Iceland only cover shallow water depths between 206 and 698m. Three species, six *D. dianthus*, five *L. pertusa*, and one *M. oculata*, show an isotope composition of  $0.28 - 0.36\text{‰}$ . The enrichment  $\Delta^{138/134}\text{Ba}_{\text{CWC-SW}}$  between seawater and coral  $\delta^{138/134}\text{Ba}$  is  $-0.16$  to  $-0.24\text{‰}$  also averaging to  $-0.19 \pm 0.05\text{‰}$ . The fractionation  $\Delta^{138/134}\text{Ba}_{\text{CWC-SW}}$  between CWCs and seawater averaged over all locations and species is  $-0.21 \pm 0.08\text{‰}$  (2SD; 2SE =  $\pm 0.01\text{‰}$ ) ( $\alpha_{\text{Ba}} = 0.99979 \pm 0.00008$ ) (Fig. 5). Averaging for each species separately leads to a Ba fractionation between  $-0.17$  and  $-0.25\text{‰}$  (Fig. 5 and supplementary material). The genus *Balanophyllia sp.* (n=5) shows the largest Ba fractionation of  $-0.25 \pm 0.05\text{‰}$  (2SD) while *Javania sp.* (n=4) fractionates Ba by only  $-0.17 \pm 0.04\text{‰}$ . The two genera with the highest variability in  $\Delta^{138/134}\text{Ba}$  were *D. dianthus* (n=9) with values ranging from  $-0.16\text{‰}$  to  $-0.28\text{‰}$  and averaging  $-0.22 \pm 0.08\text{‰}$ , and *Caryophyllia sp.* (n=8) covering a range of  $-0.16\text{‰}$  to  $-0.27\text{‰}$  and averaging  $-0.21 \pm 0.07\text{‰}$ .

## 4 Discussion

### 4.1 Constancy of $D_{\text{CWC/SW}}$ (Ba)

The mean partition coefficient derived by a linear fit to all data is  $D_{\text{CWC/SW}}(\text{Ba}) = 1.8 \pm 0.4$  (2SE, see Fig. 3a) covering a range from 1.5 to 2.4 for separate samples. These values are similar to those in previous studies (Anagnostou et al., 2011; Spooner, 2016). The study by Anagnostou et al., 2011 ( $\text{Ba}/\text{Ca}_{\text{CWC}} = 1.4 (\pm 0.3) \text{Ba}/\text{Ca}_{\text{SW}} + 0 (\pm 2)$ ) did not reveal a significant correlation between the partition coefficient and seawater temperature, salinity or pH. Spooner (2016) analysed possible environmental

impacts on  $D_{\text{CWC/SW}}(\text{Ba})$  in more detail, confirming the findings of Anagnostou et al. (2011), and indicating that  $D$  is independent of seawater nutrient content ( $\text{PO}_4$ ) and oxygen concentrations. Data in this study support the previous finding that incorporation of Ba into CWCs does not depend on seawater temperature (Fig. 7(a)), water depth, salinity, pH or nutrient content but seems to occur at a constant  $D$  value (Tab. A1 in supplementary material). Within the stated uncertainty of 0.4, no clear inter-species or location effect is resolved. Analysis at higher precession and a considerably larger data set might resolve variations smaller than the resolution here. At the stated uncertainty of 0.4, however, we consider  $D$  constant which favours the use of CWCs to reconstruct past oceanic Ba concentrations, with potential application to assess past biogeochemical cycling of Ba and/or ocean circulation.

#### 4.2 Constancy of $\Delta^{138/134}\text{Ba}_{\text{CWC-SW}}$

With a mean enrichment factor  $\Delta_{\text{BaSO}_4\text{-SW}}$  of  $-0.21 \pm 0.08\text{‰}$  (Fig. 5) all thirty-six coral samples analysed in this study are enriched in lighter Ba isotopes compared to ambient seawater (Fig. 4). The incorporation of lighter isotopes during carbonate formation is similar to other isotope systems such as Ca (e.g. Böhm et al., 2006; Fantle and DePaolo, 2007), Sr (e.g. Fietzke and Eisenhauer, 2006; Raddatz et al., 2013), Mg (e.g. Yoshimura et al., 2011) and Li (e.g. Marriott et al., 2004; Rollion-Bard et al., 2009). The most likely explanation for the fractionation is a kinetic effect combined with biological impacts (e.g. Böhm et al., 2006; DePaolo, 2004).

The offset towards light Ba isotopes during incorporation into a mineral phase is similar to that seen in limited previous studies. Pretet et al. (2016) analysed two *L. pertusa* from the Norwegian margin and found  $\delta^{138/134}\text{Ba}$  of  $0.25 \pm 0.11\text{‰}$  and  $0.3 \pm 0.11\text{‰}$ , but without accompanying seawater measurements. The coral values in that study are, however, identical within uncertainties to North Atlantic corals from this study. Further analyses in Pretet et al. (2016) on cultured tropical aragonitic scleractinian corals showed a more variable fractionation than observed here, varying between  $-0.02\text{‰}$  (*Acropora* sp. and *Porite* sp.) and  $-0.38\text{‰}$  (*Stylophora* sp. and *Montipora* sp.) (Fig. 6).

Previous inorganic precipitation experiments of  $\text{BaSO}_4$  and  $\text{BaMn}[\text{CO}_3]_2$  showed a similar preference for incorporation of lighter isotopes, with a fractionation of  $-0.33 \pm 0.04\text{‰}$  and  $-0.17 \pm 0.028\text{‰}$  respectively (Fig. 6; (von Allmen et al., 2010; Böttcher et al., 2012)). Reported Ba isotope fractionation

during  $\text{BaCO}_3$  precipitation is between  $-0.25 \pm 0.028\text{‰}$  (von Allmen et al., 2010) and  $-0.07 \pm 0.04\text{‰}$  (Mavromatis et al., 2016). The fractionation observed for CWCs analysed in this study lies roughly in the middle of the fractionation range reported on precipitates or cultured aragonite tropical corals (Fig. 6; (von Allmen et al., 2010; Böttcher et al., 2012; Pretet et al., 2016)). Analysis of the relationship between  $[\text{Ba}]$  and  $\delta^{138/134}\text{Ba}$  in seawater also suggests that Ba isotopes incorporated into  $\text{BaSO}_4$  during precipitation in the water column are lighter than seawater, with  $\Delta_{\text{BaSO}_4\text{-SW}} = -0.28 \pm 0.10\text{‰}$  (Horner et al., 2015) or  $-(0.4 - 0.5)\text{‰}$  (Bridgestock et al., 2018; Horner et al., 2017). The results in this study for coral aragonite are at the lower limit of this range.

At the precision of our measurements, there is no correlation between water temperature (between 2 and  $12^\circ\text{C}$ ) and Ba isotope fractionation ( $\Delta^{138/134}\text{Ba}$ ) observed in this study (Fig. 7(b), supplementary material). No previous study has assessed the temperature dependency of  $\Delta^{138/134}\text{Ba}$  on  $\text{CaCO}_3$  formation, although no temperature dependency of fractionation in laboratory grown  $\text{BaCO}_3$  precipitates was found (von Allmen et al., 2010). A possible effect of precipitation rates was observed for Ba fractionation into  $\text{BaCO}_3$  precipitates with a larger fractionation for slower precipitation rates. Transferring this observation to the higher variance seen in the cultured corals compared to the natural coral analysed in this study cannot explain the observed discrepancy. Known linear extension rates of the taxa analysed in this study span a wide range, from e.g.  $0.5 - 3.1 \text{ mm/a}$  for *D. dianthus* and  $5 - 26 \text{ mm/a}$  for *L. pertusa* (Gass and Roberts, 2006; Mortensen, 2001; Orejas et al., 2008), and no significant impact on Ba fractionation could be observed at the precision achieved in this study.

No substantial correlation between fractionation and nutrient availability ( $\text{PO}_4$ ) could be observed (supplementary material). Analyses of other environmental factors like depth, pH and salinity provided no clear evidence for significant impacts on Ba fractionation (supplementary material). At the precision achieved here, there is also no influence of dissolved Ba concentration in seawater on Ba isotope fractionation (Fig. 7(c)).

Different species span a range of enrichment factors from  $-0.17\text{‰}$  (*Javania* sp.) to  $-0.25\text{‰}$  (*Balanophyllia* sp.) (Fig. 5). However, this possible inter-species difference is barely resolved at the  $0.03\text{‰}$  level of our analytical uncertainty and compounded by the possibility of regional variations. All species lie well within the 2SD ( $0.08\text{‰}$ ) of the average fractionation between seawater and CWCs

( $\Delta^{138/134}\text{Ba}_{\text{CWC-SW}} = -0.21\text{‰}$ ). The isotope offset of CWCs at the Drake Passage may also be subtly different from that in the Atlantic (Fig. 4), but again any difference is very close to analytical uncertainty and lies well within the 2SD of the average fractionation. It is possible that species or local effects may become apparent with future higher precision or a significant larger data set, but at the stated uncertainty of 0.08‰ the offset between seawater and CWC Ba isotopes is constant.

#### 4.3 $\delta^{138/134}\text{Ba}$ : a new proxy for paleoceanography

Recent studies have demonstrated a strong linear relationship between  $\delta^{138/134}\text{Ba}$  and [Ba] in seawater (Bates et al., 2017; Hsieh and Henderson, 2017; Horner et al., 2015; Bridgestock et al., 2018). Local deviations from this relationship could provide evidence for local inputs of Ba with distinct isotope compositions. Variation in the nature of the global relationship may occur in the past, and would indicate changes in the global biogeochemical cycling of Ba through time. The fact that, within the uncertainties stated in this study, both  $D_{\text{CWC/SW}}(\text{Ba})$  and  $\Delta^{138/134}\text{Ba}_{\text{CWC-SW}}$  are found to be constant for CWCs regardless of the growth environment suggests that measurements on fossil corals would allow reconstruction of the past ocean relationship between [Ba] and  $\delta^{138/134}\text{Ba}$ . Analysis of coralline Ba/Ca can provide information about the [Ba] of the water the coral grew in, with possible implications for changing productivity and/or water circulation. However, measurements of this parameter alone cannot provide information about local inputs of Ba, nor possible changes in the whole oceanic Ba cycle but can be constrained by additional  $\delta^{138/134}\text{Ba}$  analyses. Thus, our observations suggest future applications regarding the reconstruction of the past marine Ba cycle using coupled Ba/Ca and Ba isotope measurements in CWCs.

Based on the data presented here we can test the potential accuracy of seawater Ba reconstructions from CWCs. The constancy of both the elemental partition coefficient and isotope fractionation for Ba in combination with the safe assumption that the seawater Ca content remained similar on long timescales, enables reconstruction of past seawater [Ba] and  $\delta^{138/134}\text{Ba}$  from coral data. Within uncertainty the reconstructed linear correlation for seawater has slope and intersect values that are equal to the relationship directly measured in seawater samples (Fig. 8).

To avoid the possibility of circular reasoning by using the same coral set to both define and test  $D_{CWC/SW}$  (Ba) and  $\Delta^{138/134}Ba_{CWC-SW}$  to reconstruct seawater, we ran repeated Monte-Carlo cross validations splitting the data set in two halves. The cross validation was run 1000 times to assess the predictive capability of our calibration for  $D_{CWC/SW}$  (Ba) and  $\Delta^{138/134}Ba_{CWC-SW}$  (supplementary material). The distribution obtained confirms the results when using all thirty-six CWCs for both the elemental partition and isotope fractionation, and slope and y-intersect of the seawater  $\delta^{138/134}Ba$ -[Ba] correlation. The average  $\delta^{138/134}Ba$  deviation of each reconstructed seawater value from the best-fit regression through the seawater observations is 0.03‰, indicating the expected uncertainty in future studies on past seawater reconstructions. This level of uncertainty is similar to the uncertainty of an individual Ba isotope analysis, suggesting that the range of values observed for the fractionation  $\Delta^{138/134}Ba_{CWC-SW}$  and partition coefficient  $D_{CWC/SW}$  (Ba) are largely due to measurement uncertainty, rather than systematic biases within the data set. Furthermore, the level of uncertainty is small relative to the observed geographical variation in the modern ocean (Fig. 2), supporting the strength of coupling Ba/Ca and Ba isotope measurements on CWCs to provide novel assessment of the past Ba cycle in the past. This approach might be used to trace changes in nutrient cycling, upwelling, and water-mass circulation (Bates et al., 2017; Bridgestock et al., 2018; Horner et al., 2015). Changes in the general relationship of  $\delta^{138/134}Ba$  and [Ba] in the past might also be used to identify whole-ocean changes in the Ba-cycle and deviations from the relationship used to assess inputs in the past ocean (e.g. from rivers or in the deep ocean) (Cao et al., 2016; Hsieh and Henderson, 2017).

## 5 Conclusions

Barium isotopes ( $\delta^{138/134}Ba$ ) in eight different taxa of colonial and solitary aragonitic scleractinian cold-water corals (CWC), taken from sites in the North Atlantic, the Equatorial Atlantic, and the Drake Passage, show a surprisingly constant isotope offset towards lighter values with a mean of  $\epsilon_{Ba} \approx \Delta^{138/134}Ba_{CWC-SW} = -0.21 \pm 0.08\text{‰}$ . Within this reproducibility no relationship with species or location and the environmental variables dissolved Ba concentration, depth, temperature, salinity, pH or phosphate concentration is observed. The mean partition coefficient for Ba ( $D_{CWC/SW}$  (Ba) =  $1.8 \pm 0.4$ ) is within the range found in previous studies, regardless of the growth environment. The constancy of

elemental partitioning and isotope fractionation indicate that coupled [Ba] and  $\delta^{138/134}\text{Ba}$  analysis in CWCs can be used to reconstruct changes in the local and global relationship between [Ba] and  $\delta^{138/134}\text{Ba}$ . New information about inputs of Ba to the ocean, and the past global oceanic cycling of Ba, might thus be gained and past changes in riverine and hydrothermal inputs to the ocean assessed.

## 6 Acknowledgements

The authors would like to thank three anonymous reviewers for their helpful and constructive comments that greatly improved this manuscript. We would also like to thank the cruise members of Nathaniel B. Palmer cruise NB1103, James Cook Cruise JC094 and the N/O Thalassa cruise ICE CTD for their assistance in retrieving the samples we worked on. We thank Tristan Horner and Stephanie Bates for the early provision of the Equatorial Atlantic seawater data. This project was supported by the European Research Council (ERC) for funding to LFR and the Deutscher Akademischer Austauschdienst (DAAD) and Heidelberg Graduate School for Fundamental Physics (HGSFP), who funded FH position during the time of this project.

## References

- Adkins, J.F., Boyle, E.A., Curry, W.B., and Lutringer, A. (2003). Stable isotopes in deep-sea corals and a new mechanism for “vital effects.” *Geochim. Cosmochim. Acta* 67, 1129–1143.
- von Allmen, K., Böttcher, M.E., Samankassou, E., and Nägler, T.F. (2010). Barium isotope fractionation in the global barium cycle: First evidence from barium minerals and precipitation experiments. *Chem. Geol.* 277, 70–77.
- Anagnostou, E., Sherrell, R.M., Gagnon, A., LaVigne, M., Field, M.P., and McDonough, W.F. (2011). Seawater nutrient and carbonate ion concentrations recorded as P/Ca, Ba/Ca, and U/Ca in the deep-sea coral *Desmophyllum dianthus*. *Geochim. Cosmochim. Acta* 75, 2529–2543.
- Bates, S.L., Hendry, K.R., Pryer, H.V., Kinsley, C.W., Pyle, K.M., Woodward, E.M.S., and Horner, T.J. (2017). Barium isotopes reveal role of ocean circulation on barium cycling in the Atlantic. *Geochim. Cosmochim. Acta*.
- Bishop, J.K.B. (1988). The barite-opal-organic carbon association in oceanic particulate matter. *Nature* 332, 341–343.
- Böhm, F., Gussone, N., Eisenhauer, A., Dullo, W.-C., Reynaud, S., and Paytan, A. (2006). Calcium isotope fractionation in modern scleractinian corals. *Geochim. Cosmochim. Acta* 70, 4452–4462.

424 Böttcher, M.E., Geprägs, P., Neubert, N., von Allmen, K., Pretet, C., Samankassou, E., and Nögler, T.F.  
 425 (2012). Barium isotope fractionation during experimental formation of the double carbonate  
 426  $\text{BaMn}[\text{CO}_3]_2$  at ambient temperature. *Isotopes Environ. Health Stud.* **48**, 457–463.

427 Bridgestock, L., Hsieh, Y.-T., Porcelli, D., Homoky, W.B., Bryan, A., and Henderson, G.M. (2018).  
 428 Controls on the barium isotope compositions of marine sediments. *Earth Planet. Sci. Lett.* **481**, 101–  
 429 110.

430 Bullen, T., and Chadwick, O. (2016). Ca, Sr and Ba stable isotopes reveal the fate of soil nutrients  
 431 along a tropical climosequence in Hawaii. *Chem. Geol.* **422**, 25–45.

432 Cao, Z., Siebert, C., Hathorne, E.C., Dai, M., and Frank, M. (2016). Constraining the oceanic barium  
 433 cycle with stable barium isotopes. *Earth Planet. Sci. Lett.* **434**, 1–9.

434 Chen, T., Robinson, L.F., Burke, A., Southon, J., Spooner, P., Morris, P.J., and Ng, H.C. (2015).  
 435 Synchronous centennial abrupt events in the ocean and atmosphere during the last deglaciation.  
 436 *Science* **349**, 1537–1541.

437 Cheng, H., Adkins, J., Edwards, R.L., and Boyle, E.A. (2000). U-Th dating of deep-sea corals. *Geochim.*  
 438 *Cosmochim. Acta* **64**, 2401–2416.

439 Chow, T.J., and Goldberg, E.D. (1960). On the marine geochemistry of barium. *Geochim. Cosmochim.*  
 440 *Acta* **20**, 192–198.

441 Copard, K., Colin, C., Douville, E., Freiwald, A., Gudmundsson, G., De Mol, B., and Frank, N. (2010). Nd  
 442 isotopes in deep-sea corals in the North-eastern Atlantic. *Quat. Sci. Rev.* **29**, 2499–2508.

443 Dehairs, F., Chesselet, R., and Jedwab, J. (1980). Discrete suspended particles of barite and the  
 444 barium cycle in the open ocean. *Earth Planet. Sci. Lett.* **49**, 528–550.

445 DePaolo, D.J. (2004). Calcium isotopic variations produced by biological, kinetic, radiogenic and  
 446 nucleosynthetic processes. *Chapter Rev. Mineral. Geochem.* **55**, 255–288.

447 Douville, E., Sallé, E., Frank, N., Eisele, M., Pons-Branchu, E., and Ayrault, S. (2010). Rapid and  
 448 accurate U–Th dating of ancient carbonates using inductively coupled plasma-quadrupole mass  
 449 spectrometry. *Chem. Geol.* **272**, 1–11.

450 Fantle, M.S., and DePaolo, D.J. (2007). Ca isotopes in carbonate sediment and pore fluid from ODP  
 451 Site 807A: The  $\text{Ca}^{2+}(\text{aq})$ –calcite equilibrium fractionation factor and calcite recrystallization rates in  
 452 Pleistocene sediments. *Geochim. Cosmochim. Acta* **71**, 2524–2546.

453 Fietzke, J., and Eisenhauer, A. (2006). Determination of temperature-dependent stable strontium  
 454 isotope ( $^{88}\text{Sr}/^{86}\text{Sr}$ ) fractionation via bracketing standard MC-ICP-MS: SR ISOTOPE FRACTIONATION.  
 455 *Geochem. Geophys. Geosystems* **7**, n/a–n/a.

456 Foster, D.A., Staubwasser, M., and Henderson, G.M. (2004).  $^{226}\text{Ra}$  and Ba concentrations in the Ross  
 457 Sea measured with multicollector ICP mass spectrometry. *Mar. Chem.* **87**, 59–71.

458 Frank, N., Montagna, P., Arnaud-Haond, and & the ICECTD shipboard scientists (2012). Cruise Report  
 459 ICECTD, Brest (FR) – Reykjavik (IS) – Ponta Delgada (PO), 11 June – 07 July 2012.



460 Gass, S.E., and Roberts, J.M. (2006). The occurrence of the cold-water coral *Lophelia pertusa*  
 461 (Scleractinia) on oil and gas platforms in the North Sea: Colony growth, recruitment and  
 462 environmental controls on distribution. *Mar. Pollut. Bull.* 52, 549–559.

463 Hathorne, E.C., Gagnon, A., Felis, T., Adkins, J., Asami, R., Boer, W., Caillon, N., Case, D., Cobb, K.M.,  
 464 Douville, E., et al. (2013). Interlaboratory study for coral Sr/Ca and other element/Ca ratio  
 465 measurements. *Geochem. Geophys. Geosystems* 14, 3730–3750.

466 Henderson, P., and Henderson, Gideon M. (2009). *The Cambridge Handbook of Earth Science Data*  
 467 (New York: Cambridge University Press).

468 Horner, T.J., Kinsley, C.W., and Nielsen, S.G. (2015). Barium-isotopic fractionation in seawater  
 469 mediated by barite cycling and oceanic circulation. *Earth Planet. Sci. Lett.* 430, 511–522.

470 Horner, T.J., Pryer, H.V., Nielsen, S.G., Crockford, P.W., Gauglitz, J.M., Wing, B.A., and Ricketts, R.D.  
 471 (2017). Pelagic barite precipitation at micromolar ambient sulfate. *Nat. Commun.* 8, 1342.

472 Hsieh, Y.-T., and Henderson, G.M. (2017). Barium stable isotopes in the global ocean: Tracer of Ba  
 473 inputs and utilization. *Earth Planet. Sci. Lett.*

474 Jeandel, C., Dupré, B., Lebaron, G., Monnin, C., and Minster, J.-F. (1996). Longitudinal distributions of  
 475 dissolved barium, silica and alkalinity in the western and southern Indian Ocean. *Deep Sea Res. Part*  
 476 *Oceanogr. Res. Pap.* 43, 1–31.

477 LaVigne, M., Hill, T.M., Spero, H.J., and Guilderson, T.P. (2011). Bamboo coral Ba/Ca: Calibration of a  
 478 new deep ocean refractory nutrient proxy. *Earth Planet. Sci. Lett.* 312, 506–515.

479 LaVigne, M., Grottoli, A.G., Palardy, J.E., and Sherrell, R.M. (2016). Multi-colony calibrations of coral  
 480 Ba/Ca with a contemporaneous in situ seawater barium record. *Geochim. Cosmochim. Acta* 179,  
 481 203–216.

482 Lea, D.W., and Boyle, E.A. (1993). Determination of carbonate-bound barium in foraminifera and  
 483 corals by isotope dilution plasma-mass spectrometry. *Chem. Geol.* 103, 73–84.

484 Mangini, A., Lomitschka, M., Eichstadter, R., Frank, N., Vogler, S., Bonani, G., Hajdas, I., and Patzold, J.  
 485 (1998). Coral provides way to age deep water. *Nature* 392, 347–348.

486 Margolin, A.R., Robinson, L.F., Burke, A., Waller, R.G., Scanlon, K.M., Roberts, M.L., Auro, M.E., and  
 487 van de Flierdt, T. (2014). Temporal and spatial distributions of cold-water corals in the Drake Passage:  
 488 Insights from the last 35,000 years. *Deep Sea Res. Part II Top. Stud. Oceanogr.* 99, 237–248.

489 Marriott, C.S., Henderson, G.M., Belshaw, N.S., and Tudhope, A.W. (2004). Temperature dependence  
 490 of  $\delta^7\text{Li}$ ,  $\delta^{44}\text{Ca}$  and Li/Ca during growth of calcium carbonate. *Earth Planet. Sci. Lett.* 222, 615–624.

491 Mavromatis, V., van Zuilen, K., Purgstaller, B., Baldermann, A., Nägler, T.F., and Dietzel, M. (2016).  
 492 Barium isotope fractionation during witherite ( $\text{BaCO}_3$ ) dissolution, precipitation and at equilibrium.  
 493 *Geochim. Cosmochim. Acta* 190, 72–84.

494 Miyazaki, T., Kimura, J.-I., and Chang, Q. (2014). Analysis of stable isotope ratios of Ba by double-  
 495 spike standard-sample bracketing using multiple-collector inductively coupled plasma mass  
 496 spectrometry. *J. Anal. At. Spectrom.* 29, 483.

497 Monnin, C., Jeandel, C., Cattaldo, T., and Dehairs, F. (1999). The marine barite saturation state of the  
 498 world's oceans. *Mar. Chem.* 65, 253–261.

499 Mortensen, P.B. (2001). Aquarium observations on the deep-water coral *Lophelia pertusa* (L., 1758)  
 500 (scleractinia) and selected associated invertebrates. *Ophelia* 54, 83–104.

501 Nan, X., Wu, F., Zhang, Z., Hou, Z., Huang, F., and Yu, H. (2015). High-precision barium isotope  
 502 measurements by MC-ICP-MS. *J Anal Spectrom* 30, 2307–2315.

503 Okai, T., Suzuki, A., Kawahata, H., Terashima, S., and Imai, N. (2002). Preparation of a New Geological  
 504 Survey of Japan Geochemical Reference Material: Coral JCp-1. *Geostand. Newsl.* 26, 95–99.

505 Orejas, C., Gori, A., and Gili, J.M. (2008). Growth rates of live *Lophelia pertusa* and *Madrepora*  
 506 *oculata* from the Mediterranean Sea maintained in aquaria. *Coral Reefs* 27, 255–255.

507 Paytan, A., and Griffith, E.M. (2007). Marine barite: Recorder of variations in ocean export  
 508 productivity. *Deep Sea Res. Part II Top. Stud. Oceanogr.* 54, 687–705.

509 Pretet, C., van Zuilen, K., Nägler, T.F., Reynaud, S., Böttcher, M.E., and Samankassou, E. (2016).  
 510 Constraints on barium isotope fractionation during aragonite precipitation by corals. *Depositional*  
 511 *Rec.* 1, 118–129.

512 Raddatz, J., Liebetrau, V., Rüggeberg, A., Hathorne, E., Krabbenhöft, A., Eisenhauer, A., Böhm, F.,  
 513 Vollstaedt, H., Fietzke, J., López Correa, M., et al. (2013). Stable Sr-isotope, Sr/Ca, Mg/Ca, Li/Ca and  
 514 Mg/Li ratios in the scleractinian cold-water coral *Lophelia pertusa*. *Chem. Geol.* 352, 143–152.

515 Raddatz, J., Liebetrau, V., Trotter, J., Rüggeberg, A., Flögel, S., Dullo, W.-C., Eisenhauer, A., Voigt, S.,  
 516 and McCulloch, M. (2016). Environmental constraints on Holocene cold-water coral reef growth off  
 517 Norway: Insights from a multiproxy approach. *Paleoceanography* 31, 2016PA002974.

518 Roberts, J.M., Wheeler, A.J., and Freiwald, A. (2006). Reefs of the Deep: The Biology and Geology of  
 519 Cold-Water Coral Ecosystems. *Science* 312, 543–547.

520 Roberts, J.M., Wheeler, A.J., Freiwald, A., and Cairns, S.D. (2009). Cold-Water Corals – The Biology  
 521 and Geology of Deep-Sea Coral Habitats (Cambridge University Press).

522 Robinson, L.F. (2014). RRS James Cook Cruise JC094, October 13–November 30 2013, Tenerife-  
 523 Trinidad. TROPICS, Tracing Oceanic Processes using Corals and Sediments. Reconstructing abrupt  
 524 Changes in Chemistry and Circulation of the Equatorial Atlantic Ocean: Implications for global Climate  
 525 and deep-water Habitats.

526 Robinson, L.F., and Waller, R.G. (2011). Historic perspectives on climate and biogeography from  
 527 deep-sea corals in the Drake Passage.' Cruise report RVIB Nathaniel B Palmer Cruise 11–03, May 09–  
 528 June 2011.

529 Robinson, L.F., Adkins, J.F., Frank, N., Gagnon, A.C., Prouty, N.G., Brendan Roark, E., and de Fliertdt, T.  
 530 van (2014). The geochemistry of deep-sea coral skeletons: A review of vital effects and applications  
 531 for palaeoceanography. *Deep Sea Res. Part II Top. Stud. Oceanogr.* 99, 184–198.

532 Rollion-Bard, C., Vigier, N., Meibom, A., Blamart, D., Reynaud, S., Rodolfo-Metalpa, R., Martin, S., and  
 533 Gattuso, J.-P. (2009). Effect of environmental conditions and skeletal ultrastructure on the Li isotopic  
 534 composition of scleractinian corals. *Earth Planet. Sci. Lett.* 286, 63–70.

535 Spooner, P.T. (2016). Investigating the use of Cold-Water Corals as Archives of Past Ocean Water  
536 Properties. University of Bristol.

537 Spooner, P.T., Guo, W., Robinson, L.F., Thiagarajan, N., Hendry, K.R., Rosenheim, B.E., and Leng, M.J.  
538 (2016). Clumped isotope composition of cold-water corals: A role for vital effects? *Geochim.*  
539 *Cosmochim. Acta* *179*, 123–141.

540 Wolgemuth, K., and Broecker, W.S. (1970). Barium in sea water. *Earth Planet. Sci. Lett.* *8*, 372–378.

541 Yoshimura, T., Tanimizu, M., Inoue, M., Suzuki, A., Iwasaki, N., and Kawahata, H. (2011). Mg isotope  
542 fractionation in biogenic carbonates of deep-sea coral, benthic foraminifera, and hermatypic coral.  
543 *Anal. Bioanal. Chem.* *401*, 2755–2769.

544 van Zuilen, K., Müller, T., Nägler, T.F., Dietzel, M., and Küsters, T. (2016). Experimental determination  
545 of barium isotope fractionation during diffusion and adsorption processes at low temperatures.  
546 *Geochim. Cosmochim. Acta* *186*, 226–241.

547

548

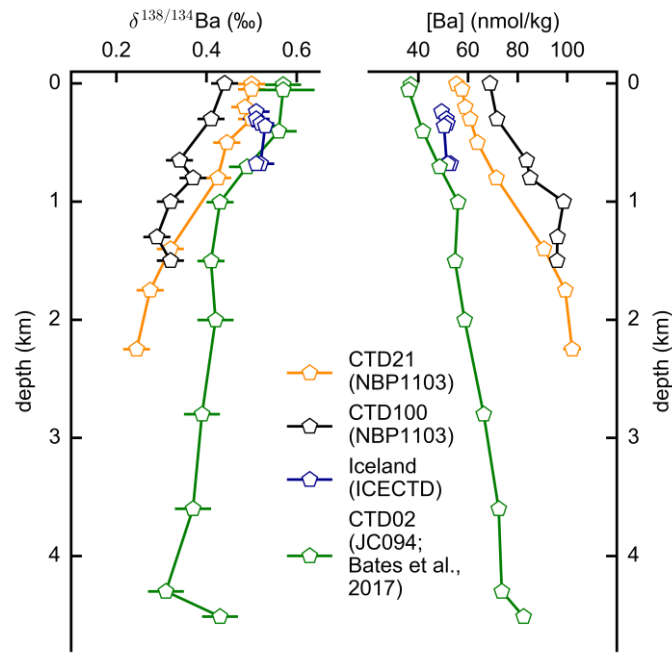


Figure 1

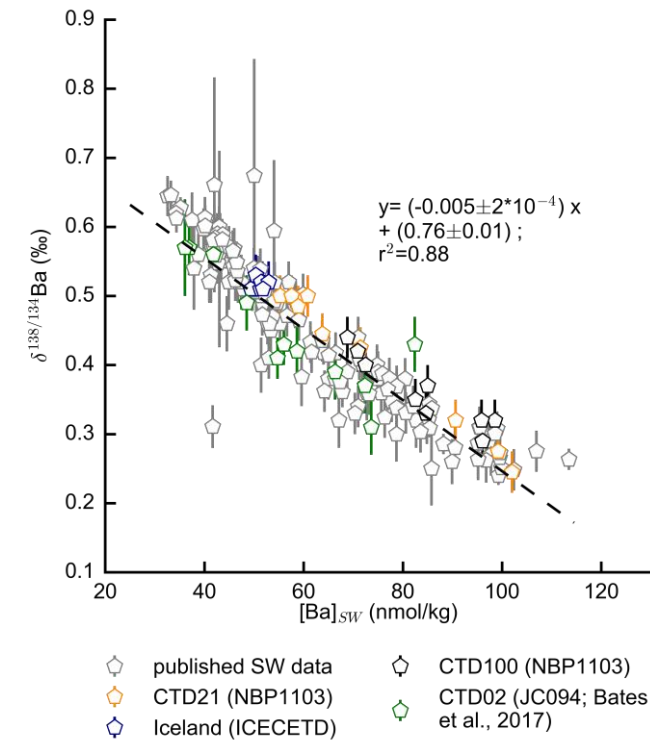
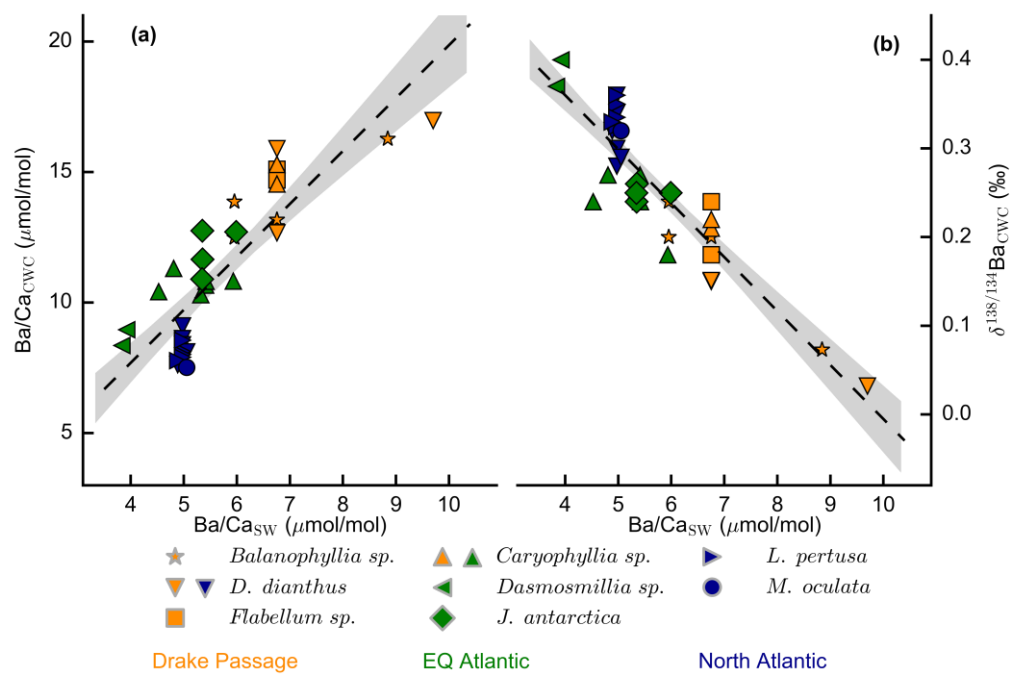


Figure 2



556

557 Figure 3

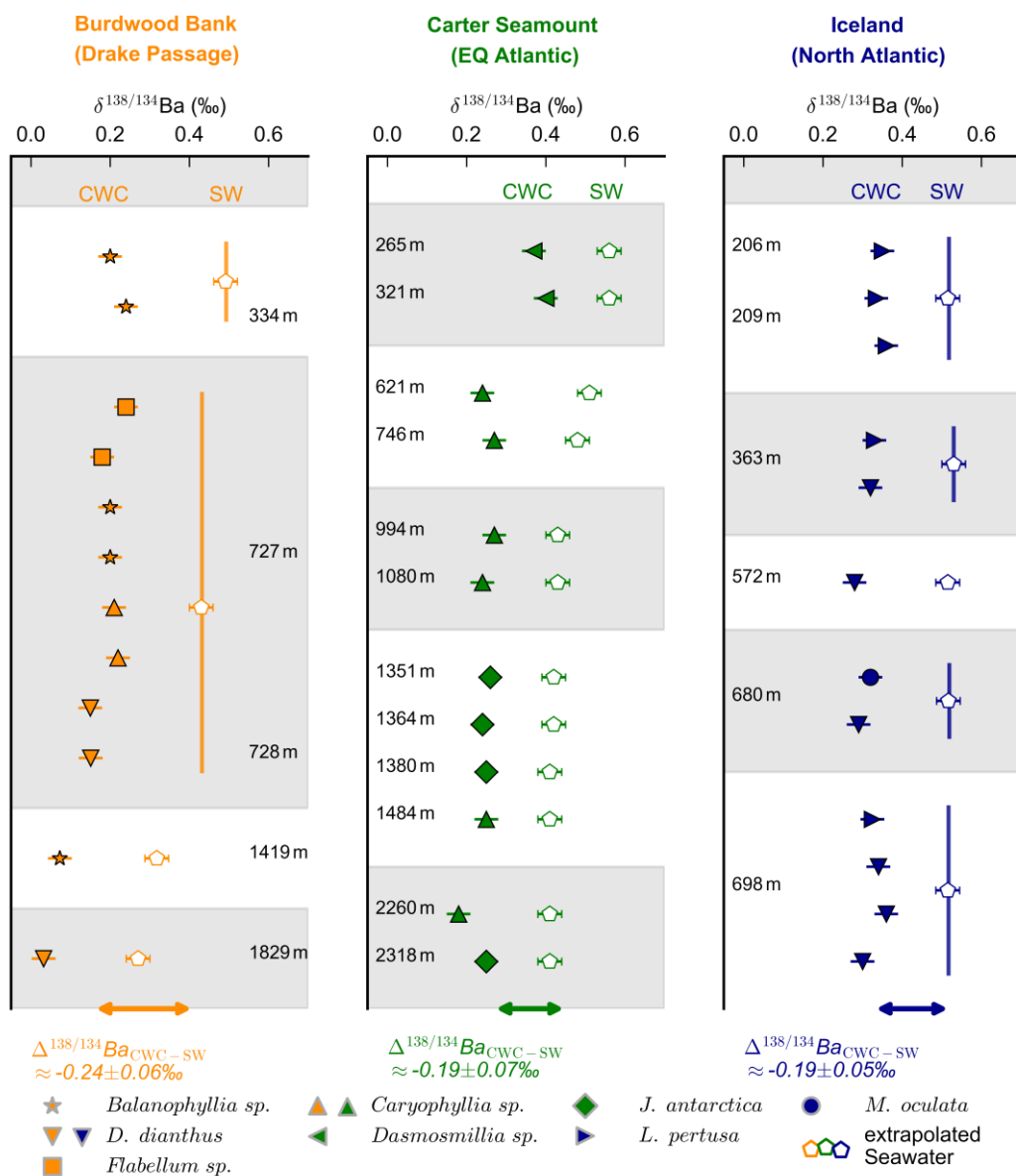


Figure 4

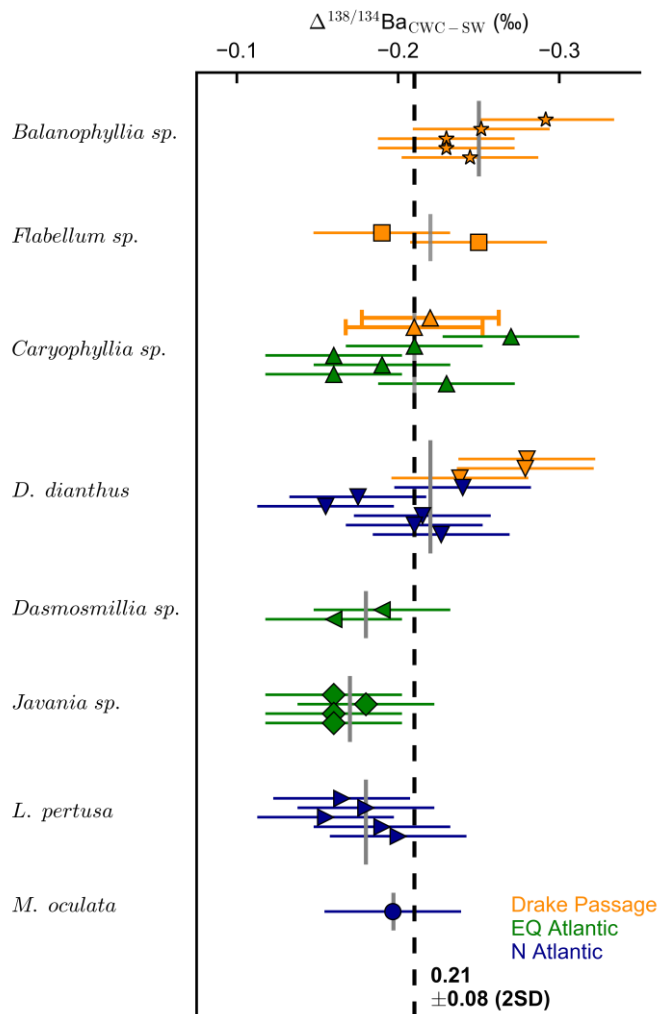


Figure 5

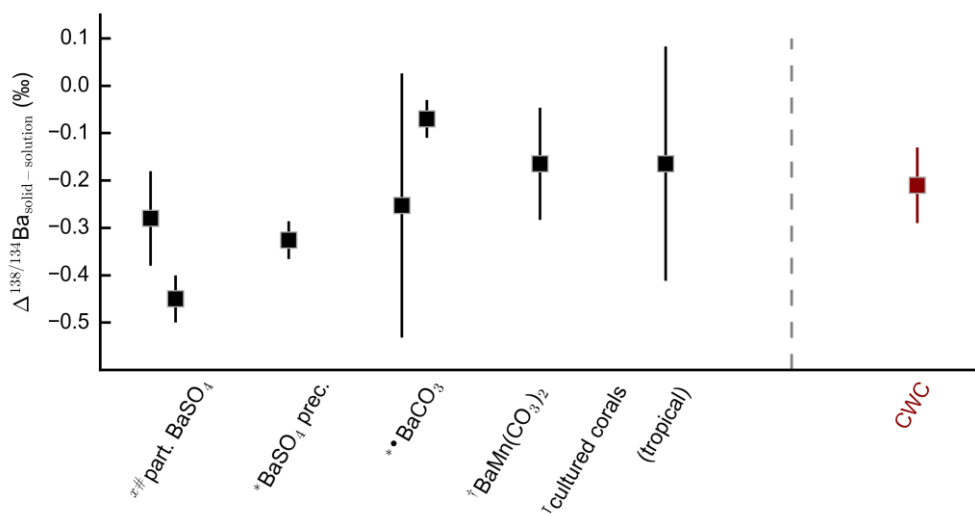


Figure 6

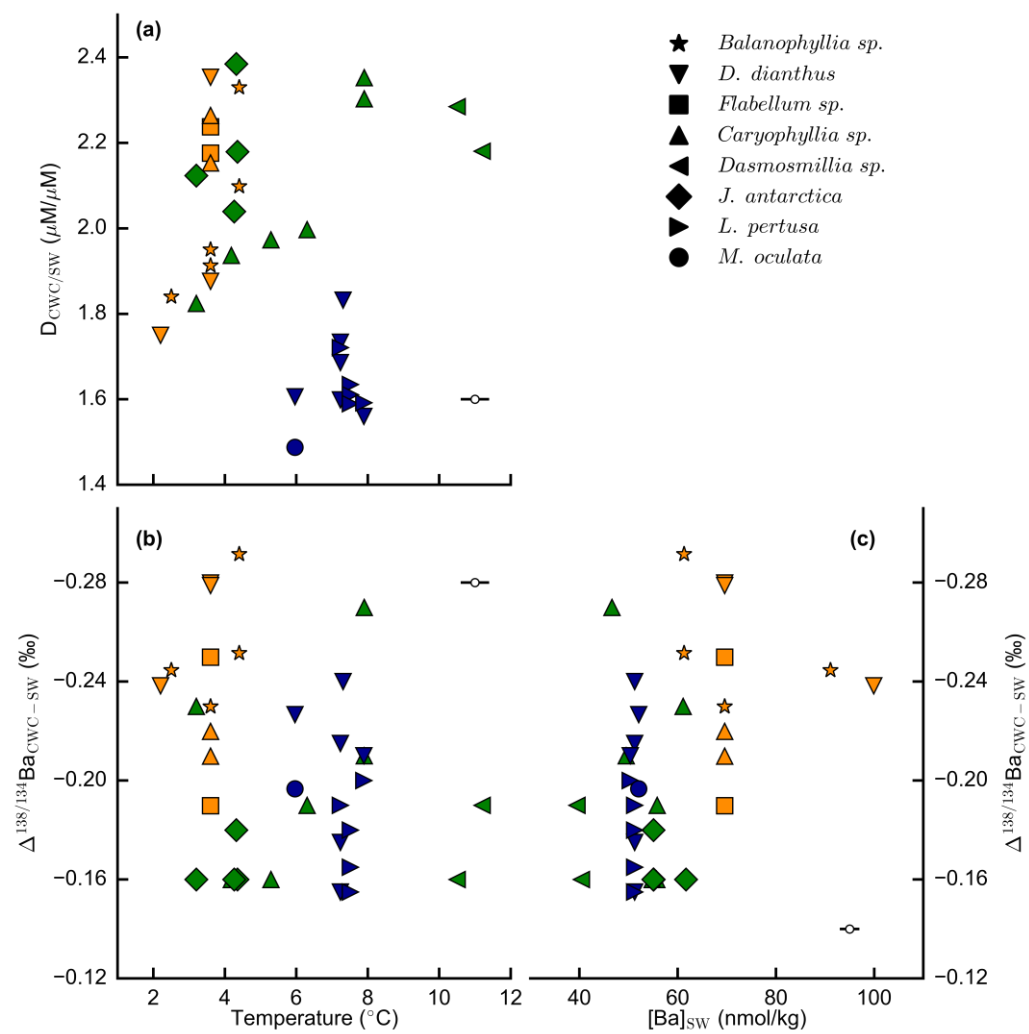


Figure 7



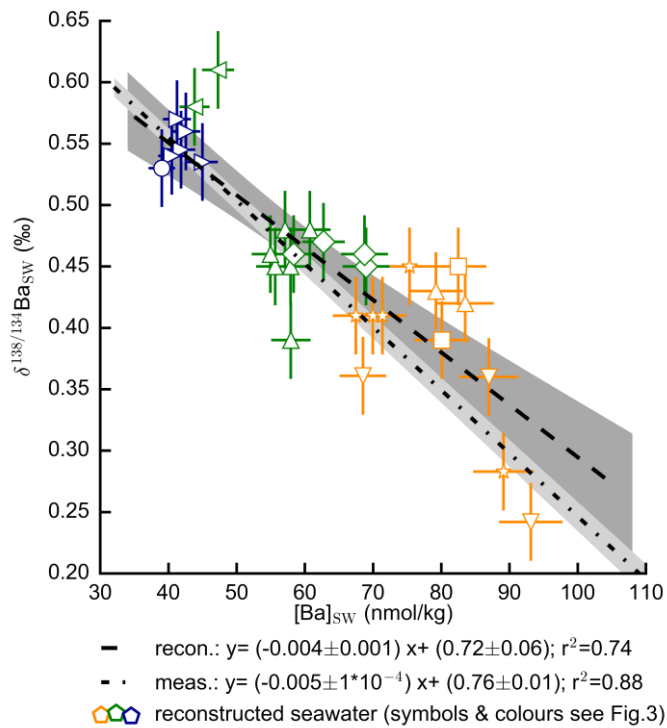


Figure 8

Table 1

station	latitude	longitude	covered depths	analysed depths (m)
Iceland				
Hafadjup CWC	63° 16.82' – 63° 20.52'N	19° 34.11' – 19° 35.75'W	363 – 680	363 – 680
Hafadjup SW	63° 19.02' N	19° 36.72'W	360 – 680	360 – 680
Reykjanes Ridge CWC	62° 36.45' – 63° 5.13'N	24° 59.27' – 24° 32.53'W	209 – 698	209 – 698
Reykjanes Ridge SW	62° 53.34'N	24° 50.88'W	238 – 338	238 – 338
Equatorial Atlantic				
Carter Seamount CWC	5° 36.66' – 9° 13.37'N	21° 16.49' – 26° 57.46' W	265 – 2318	265 – 2318
JC094 CTD 2 SW	9° 17.1'N	21° 38.0' W	0 – 4524	0 – 4524
Drake Passage				
Burdwood Bank	54° 50.26' – 54° 50.33'S	62° 7.11' – 62° 14.99'W	334 – 1829	334 – 1829
NBP1103 CTD 21	55° 3.25' S	62° 81' W	0 – 4110	0 – 2250
NBP1103 CTD 100	60° 33.85' S	65° 29.57' W	0 – 3100	0 – 1500

## Figure and table captions

### Figure 1:

Seawater profiles for dissolved Ba concentrations [Ba] and Ba isotope compositions  $\delta^{138/134}\text{Ba}$ . At all locations, station CTD21 (Burdwood Bank, orange), CTD100 (Sars Seamount, black), Iceland (Reykjanes Ridge and Hafadju, blue), and CTD02 (Carter Seamount) (Bates et al., 2017), the well-established anti-correlation between [Ba] and  $\delta^{138/134}\text{Ba}$  can be observed. Both profiles from cruise NBP1103 reach deeper, but were not analysed in abyssal depths as only depths with coral growth were considered for this study. Station CTD100 will not be discussed further as corals from Sars seamount were not analysed here.

### Figure 2:

$\delta^{138/134}\text{Ba}_{\text{sw}}$  against  $[\text{Ba}]_{\text{sw}}$  for samples from this study and published data (Bridgestock et al., 2018; Hsieh and Henderson, 2017; Bates et al., 2017; Pretet et al., 2016; Horner et al., 2015). Data from Bates et al. (2017) were used in this study for considerations of corals from the Equatorial Atlantic (green symbols). Cao et al. (2016) data were not included in this summary as their seawater samples exhibited a different correlation with higher Ba isotope compositions. Our data agree well with the other studies. Note that seawater Ba isotope composition at the coral sites cover nearly the total observed range of  $\delta^{138/134}\text{Ba}$  reported in the other studies.

### Figure 3:

Ba/Ca in CWCs and ambient seawater (a) and seawater Ba/Ca<sub>sw</sub> influence on coralline  $\delta^{138/134}\text{Ba}$  (b). (a) A linear fit (black dashed line) through the data gives:  $\text{Ba}/\text{Ca}_{\text{CWC}} = 1.8 (\pm 0.4) \text{ Ba}/\text{Ca}_{\text{sw}} + 0.7 (\pm 2.6)$  with a correlation factor of  $r^2 = 0.67$  (0.95 confidence interval as shaded grey area). (b) Similar to seawater  $\delta^{138/134}\text{Ba}$ , a close anti-correlation to Ba concentration (here as Ba/Ca<sub>sw</sub>) can be observed for coralline  $\delta^{138/134}\text{Ba}$ . The correlation factor  $r^2$  is 0.82.

### Figure 4:

$\delta^{138/134}\text{Ba}$  in CWCs (filled symbols) at all three sites compared to ambient seawater (open symbols). Seawater values are extrapolated to the depth each coral grew at. All CWCs are isotopically lighter than ambient seawater, with higher Ba isotope compositions in shallower depths than in deeper waters. Within uncertainties all sites show a similar mean fractionation. The overall fractionation of Burdwood Bank corals is  $\Delta^{138/134}\text{Ba}_{\text{CWC-SW}} = -0.24 \pm 0.06\text{‰}$ , while Carter Seamount and Iceland corals both fractionate Ba by  $-0.19\text{‰}$  with a 2SD of  $\pm 0.07\text{‰}$  and  $\pm 0.05\text{‰}$  respectively.

Figure 5:

$\Delta^{138/134}\text{Ba}_{\text{CWC}}$  for each species/ genus separately.

The overall fractionation between corals and seawater is  $\Delta^{138/134}\text{Ba}_{\text{CWC}} = -0.21 \pm 0.08\text{‰}$  (2SD and  $0.01\text{‰}$  SE). The maximum species specific fractionation is  $\Delta^{138/134}\text{Ba}_{\text{CWC}} = -0.25 \pm 0.05\text{‰}$  for *Balanophyllia* sp. and the minimum  $\Delta^{138/134}\text{Ba}_{\text{CWC}} = -0.17 \pm 0.04\text{‰}$  for *Javania* sp. (uncertainties are the larger of external reproducibility and 2SD from averaging). The species *D. dianthus* shows the largest variability in  $\Delta^{138/134}\text{Ba}_{\text{CWC}}$ , ranging from  $-0.16$  to  $-0.28\text{‰}$  and an average of  $-0.22 \pm 0.08\text{‰}$ .

Figure 6:

Comparison of  $\Delta^{138/134}\text{Ba}$  to published assessments. Particulate  $^{138}\text{BaSO}_4$  (part.) were estimated by Horner et al., 2015,  $^{138}\text{BaSO}_4$  (part.) by Bridgestock et al., 2018 and Horner et al., 2017, precipitates of  $^{138}\text{BaSO}_4$  (prec.) and  $^{138}\text{BaCO}_3$  were analysed by von Allmen et al., 2010, of  $^{138}\text{BaCO}_3$  by Mavromatis et al., 2016, of  $^{138}\text{BaMn}[\text{CO}_3]_2$  by Böttcher et al., 2012 and  $^{138}\text{Ba}$  cultured tropical corals were investigated by Pretet et al., 2016. Uncertainties are 2SE for repeat analysis of one sample.

The variation seen in precipitates is larger than for all thirty-six natural CWCs investigated in this study (red). CWCs are separately analysed for location and species in Fig. 4 and 5.

Figure 7:

Temperature dependency of  $D_{\text{CWC/SW}}$  (a) and  $\Delta^{138/134}\text{Ba}_{\text{CWC}}$  (b), and correlation between  $[\text{Ba}]_{\text{SW}}$  and  $\Delta^{138/134}\text{Ba}_{\text{CWC}}$  (c). No correlation of  $D_{\text{CWC/SW}}$  with temperature ( $r^2 = 0.02$ ) and  $\Delta^{138/134}\text{Ba}_{\text{CWC}}$  with

temperature ( $r^2 = 0.12$ ) and  $[\text{Ba}]_{\text{sw}}$  ( $r^2 = 0.16$ ) can be observed (for colours see e.g. Fig. 4). Uncertainties for temperature and  $[\text{Ba}]_{\text{sw}}$  are displayed with the extra open data point.

Figure 8:

Comparison between the established seawater  $[\text{Ba}]_{\text{sw}}$  and  $\delta^{138/134}\text{Ba}$  correlation (meas.: dash-dot line) and the seawater characteristic 'reconstructed' from the CWCs (reconstructed: dashed line). The reconstruction was achieved by applying a constant partition coefficient and isotope fractionation for Ba to the measured CWC data, obtaining the open coloured symbols (for symbols see e.g. Fig. 3). Uncertainties shown are the external reproducibilities from our measurements. Within uncertainties (grey envelopes) the 'reconstructed' seawater data and  $[\text{Ba}]_{\text{sw}}$  and  $\delta^{138/134}\text{Ba}$  correlation agree with the well-known seawater anti-correlation for  $[\text{Ba}]_{\text{sw}}$  and  $\delta^{138/134}\text{Ba}$ .

Table 1:

Locations of CWC and seawater sample sites. For the exact coordinates of each cold water coral please refer to the supplementary material.